

## A New Equation for Predicting Electrical Conductivity of Carbon-Filled Polymer Composites Used for Bipolar Plates of Fuel Cells

Reza Taherian,<sup>1</sup> Mohammad Jaffar Hadianfard,<sup>2</sup> Ahmad Nozad Golikand<sup>1</sup>

<sup>1</sup>Material Research Center, Tehran, Iran

<sup>2</sup>Material Engineering Department, Shiraz University, Shiraz, Iran

Correspondence to: R. Taherian (E-mail: Iran rezataherian@gmail.com)

**ABSTRACT:** In this article, a statistical-thermodynamic formula based on a new approach has been developed to predict electrical conductivity of carbon-filled composites used for bipolar plate of proton exchange membrane fuel cell. In this model, based on percolation threshold phenomenon, it is assumed that the relationship between electrical conductivity of composite and filler volume fraction follows a sigmoidal equation. Afterwards, the four effective factors on composite conductivity including filler electrical conductivity, filler aspect ratio, wettability, as well as interface contact resistance are replaced upon constant parameters of sigmoidal function. In order to test the model, some single-filler composites have been manufactured by using the phenolic resin as binder and graphite (G), expanded graphite (EG), and carbon fiber (CF) as fillers. The fitting quality is measured by *R*-square, adjusted *R*-square, SSE, and RMSE parameters. The results showed that there is a noteworthy agreement between the model and the experimental data. Compared to the other models, this model can be used for more types of fillers. © 2012 Wiley Periodicals, Inc. *J. Appl. Polym. Sci.* 000: 000–000, 2012

**KEYWORDS:** electrical conductivity; model; composite; polymer; carbon

Received 8 May 2012; accepted 22 June 2012; published online

DOI: 10.1002/app.38295

### INTRODUCTION

Fuel cells have been proposed as a clean energy source, which can be utilized to power vehicles. A typical fuel cell in an automotive application can contain hundreds of bipolar plates, which consists of an electrically conductive material.<sup>1</sup> Currently, 70–90 weight percent of a single type of graphite powder in a thermosetting resin is typically being used for bipolar plates.<sup>2</sup> Metallic plates have been utilized but these have several disadvantages relative to conductive resins including higher cost, weight, and less corrosion resistance. Pure graphitic bipolar plates also have some disadvantages such as poor mechanical properties, poor machining, and high hydrogen permeability. Polymers are naturally insulating materials. Their electrical conductivity can be enhanced by the addition of electrically conductive carbon fillers.<sup>3,4</sup> Typically, polymers exhibit electrical conductivities in the range of  $10^{-14}$ – $10^{-17}$  S/cm. Electrical conductivities of typical conductive carbon fillers range from  $10^2$  to  $10^5$  S/cm. The combination of a polymer and electrically conductive filler(s) may result in an electrically conductive resin effective for fuel cell bipolar plate applications. An electrical conductivity target value for an effective bipolar plate has been prescribed by Department of Energy of USA (DOE) for the second generation fuel cell systems to be  $>10^2$  S/cm.<sup>5</sup> A correlation exists between the electrical conductivity of the various polymer

composites and the carbon filler concentration of the composite (Figure 1). At low filler loadings, the electrical conductivity is equivalent to the electrical conductivity of the insulating polymer. As Figure 1 shows, in the low filler loading, the fillers are dispersed throughout the insulated matrix. In this region, the conductive network is not completed and there are not enough conductive pathways throughout the composite and therefore, the conductivity mechanism is usually tunneling effect. As the filler concentration increases, the first continuous chains from conductive fillers are initiated. The region that the electrical conductivity is magnified by several orders of magnitude at a critical volume fraction is called the percolation threshold. Upon further increase of the carbon filler content, the number of continuous chains increases. In this region, the electrical conductivity only shows a slight increase until a plateau is observed.<sup>7</sup>

Various models have been proposed to predict the electrical conductivity behavior of composites based on numerous factors (Table I). Although all the models base calculations on the filler volume fraction, there are other factors that can affect the conductivity of the composite such as polymer wettability, contact resistance between filler particles, and filler aspect ratio. Physical properties of both the filler and polymer will influence the composite and include structural properties, interfacial properties,

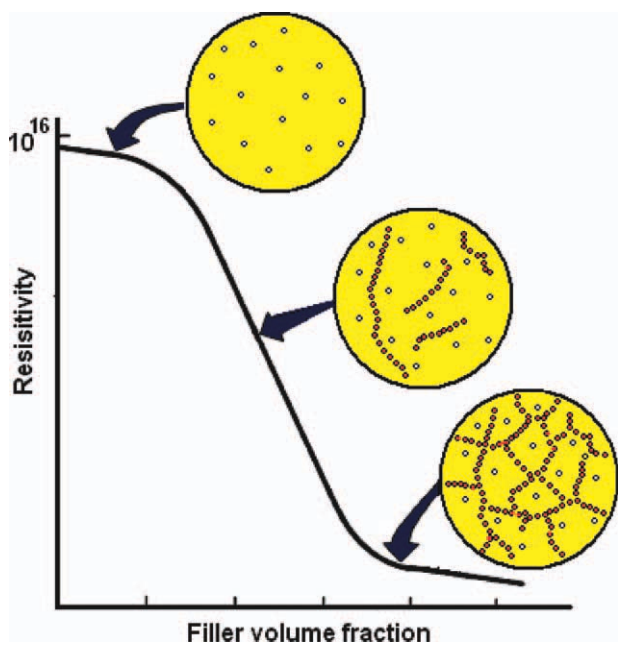


**Figure 1.** Description of conductive network formation through the carbon filled composite ( $\rho$  and  $v_f$  are the inherent electrical resistivity of composite and the filler volume percentage, respectively).<sup>6</sup> [Color figure can be viewed in the online issue, which is available at [wileyonlinelibrary.com](http://wileyonlinelibrary.com).]

and constituent conductivity. The properties of the filler that play a significant role in determining the conductivity of the composite include filler type, size, and shape. The forms of carbon generally differ from one another in structure, morphology, purity, and thereby electrical conductivity. In addition, particle size and aspect ratio of filler can greatly affect the electrical conductivity of the composite. It was reported that for spherical particles, the smaller particle size will lower the percolation threshold,<sup>17</sup> while for particles with an aspect ratio (ratio of length to diameter,  $L/D$ ) greater than 1, larger aspect ratios and a broader range of aspect ratios will lower the percolation threshold.<sup>18–20</sup> The surface properties of the filler and polymer also have a significant effect on the conductivity of the composite<sup>21</sup> by influencing the interaction between them. How well the polymer wets the surface of the filler can be quantified by the difference between the surface energies of the two materials.<sup>11</sup> Due to the distinct influence of mentioned parameters on a composite system, four main classes of conductivity models have been developed which can be found in the literature. They include statistical, thermodynamic, geometrical, and structure-oriented models, as described in detail by Lux.<sup>22</sup> Each class predicts the electrical conductivity based on distinct approaches to account for the parameters described above.

### Statistical Percolation Models

Most of the models found in the literature are of the statistical percolation type. These models typically predict the conductivity based on the probability of particle contacts within the composite. Two of the early percolation models often referenced were originally proposed by Kirkpatrick<sup>8</sup> and Zallen.<sup>23</sup> The model that was proposed followed a power-law equation of the following form:

$$\sigma = \sigma_0(V - V_c)^s \quad (1)$$

where  $\sigma$  is the conductivity of the mixture;  $\sigma_0$ , the conductivity of the filler;  $V$ , the volume fraction of the filler;  $V_c$ , the volume percolation fraction; and  $s$ , the critical exponent which depends upon the dimension of the lattice. This particular model was not completely accurate in calculating the electrical conductivity, because this model cannot predict the electrical conductivity before percolation threshold. However, it has become the basis for many of the later conductivity models. Bueche<sup>23</sup> tried to explain the problem of conductive particles in an insulating matrix based on the concept of polymer gelation. The resulting equation is given by:

$$\rho = \frac{\rho_m \rho_f}{(1 - V_f)\rho_f + V_f \omega_g \rho_m} \quad (2)$$

where  $\rho$  is the resistivity of the mixture;  $\rho_m$ , the resistivity of the insulator;  $\rho_f$ , the resistivity of the conductor;  $V_f$ , the volume fraction of the conductive phase; and  $\omega_g$ , the weight fraction of the conductive phase in an infinite cluster, a function of the number of contacts per particle and the probability of contact.

Another example of an improved statistical model was proposed by McLachlan et al.<sup>9</sup> McLachlan et al. suggested that this particular model could be used for any system comprising a high conductivity material embedded in a poorly conducting material. This model is given by:

$$\frac{(1 - \phi)(\rho_m^{1/t} - \rho_h^{1/t})}{\rho_m^{1/t} + \left(\frac{1 - \phi_c}{\phi_c}\right)\rho_h^{1/t}} + \frac{\phi(\rho_m^{1/t} - \rho_l^{1/t})}{\rho_m^{1/t} + \left(\frac{1 - \phi_c}{\phi_c}\right)\rho_l^{1/t}} \quad (3)$$

where  $\rho_m$  is the resistivity of the composite;  $\rho_h$ , the resistivity of the component with high resistivity;  $\rho_l$ , the resistivity of the component with low resistivity;  $\phi$ , the volume fraction;  $\phi_c$ , the percolation threshold; and  $t$ , the critical exponent.

### Thermodynamic Models

Mamunya et al.<sup>11,12</sup> studied the composite conductivity versus the filler volume fraction for different polymers in a way that allowed them to evaluate the influence of other factors on the conductivity. These factors included filler and polymer surface energies and polymer melt viscosity, among others. By considering these particular factors, this model fits into the thermodynamic model category. The resulting model showed that the percolation behavior was dependent on the polymer–filler interaction, in addition to the size and amount of the filler material. At all points above the percolation threshold, the conductivity of the composite was found to be:

$$\log \sigma = \log \sigma_c + (\log \sigma_m - \log \sigma_c) \left( \frac{\phi - \phi_c}{F - \phi_c} \right)^k \quad (4)$$

$$k = \frac{K\phi_c}{(\phi - \phi_c)^{0.75}}, \quad K = A - B\gamma_{pt} \quad (5)$$

where  $\sigma$  is the composite conductivity;  $\sigma_c$ , the conductivity at the percolation threshold;  $\sigma_m$ , the conductivity at  $F$ ;  $F$ , the

**Table I.** Description of Some of the Common Models

1. Kirkpatrick and Zallen <sup>8</sup>	$\sigma_m = \sigma_h(\phi - \phi_c)^t$
2. McLachlan <sup>9,10</sup>	$\frac{(1 - \phi)(\rho_m^{1/t} - \rho_h^{1/t})}{\rho_m^{1/t} + (\frac{1-\phi_c}{\phi_c})\rho_h^{1/t}} + \frac{\phi(\rho_m^{1/t} - \rho_f^{1/t})}{\rho_m^{1/t} + (\frac{1-\phi_c}{\phi_c})\rho_f^{1/t}} = 0$
3. Mamunya et al. <sup>11,12</sup>	$\log \sigma_m = \log \sigma_c (\log \sigma_f \log \sigma_c) (\frac{\phi - \phi_c}{F - \phi_c})^k$ $F = \frac{5}{\frac{75}{10+AR} + AR}$ $k = \frac{K\phi_c}{(\phi - \phi_c)^{0.75}}$ $K = A - B\gamma_{pf}$ $\gamma_{pf} = \gamma_p + \gamma_f - 2(\gamma_p\gamma_f)^{0.5}$
4. Clingerman (Additive Model) <sup>13</sup>	$\log \sigma_m = \log \sigma_p, \text{ for } \phi \leq \phi_c$ $\log \sigma_m = \log \sigma_p + D \log \sigma_f (\phi - \phi_c)^q + h(a) \cos \theta - C\gamma_{pf},$ $\text{for } \phi > \phi_c$ $q = \frac{B\phi_c}{(\phi - \phi_c)^N}$ $h(a) = A^2 [1 - 0.5(A - 1/A) \times \ln[(A + 1)/(A - 1)]]$ $A^2 = \frac{a^2}{a^2 - 1}$
5. Keith <sup>1</sup>	$\log \sigma = \log \sigma_p + H(\phi - \phi_c)^{\frac{G}{(\phi - \phi_c)^n}} + E$
6. Nielsen <sup>14</sup>	$\sigma_m = \sigma_p \cdot \frac{1 + AB\phi}{1 - B\Psi\phi}$ $B = \frac{\frac{\sigma_h}{\sigma_f} - 1}{\frac{\sigma_h}{\sigma_p} + A}$ $\Psi \approx 1 + \left(\frac{1 - F}{F^2}\right) \cdot \phi$
7. McCullough <sup>6</sup>	$P_i = \phi_f P_f + \phi_m P_p - \left[ \frac{\lambda_i \phi_f \phi_m (P_f - P_p)^2}{V_{fi} P_f + V_{mi} P_p} \right]$ $V_{fi} = (1 - \lambda_i) \phi_f + \lambda_i \phi_m$ $V_{mi} = (1 - \lambda_i) \phi_m + \lambda_i \phi_f$
8. Contact model <sup>6,15</sup>	$\rho_{c, \text{long}} = \frac{\pi d^2 \rho_f X}{4\phi d_c \ell \cos^2 \theta_a}$
9. Weber <sup>6,15</sup>	$\sigma_c = \sigma_m + [4/\pi \left( d_c \cdot \frac{l}{d^2 \cos^2 \phi} \right) (v_p \sigma_f) X]$ $X = 1/(0.59 + 0.15m)$
10. Voet <sup>16</sup>	$\log \sigma = K\phi^{1/3}$
11. Scarisbrick <sup>16</sup>	$\frac{\sigma_c}{\sigma_f} = \phi \times \phi [\exp(\phi^{-\frac{2}{3}})] \times C^2$

$\sigma_m$ : electrical conductivity of composite,  $\sigma_h$  or  $\sigma_f$ : filler conductivity,  $\phi$ : filler volume fraction,  $\phi_c$ : filler volume fraction in percolation threshold,  $\rho_h$ : filler resistivity,  $\rho_f$ : polymer resistivity,  $t$ : critical exponent,  $\sigma_c$ : conductivity in maximum volume fraction ( $F$ ),  $F$ : compact factor,  $\gamma$ : surface energy,  $\sigma_p$ : polymer conductivity,  $\theta$ : wetting angle,  $a$ : aspect ratio,  $\gamma_{pf}$ : interface surface energy,  $m$ : contact number between fillers,  $d$ : filler diameter,  $d_c$ : critical filler diameter,  $l$ : filler length,  $\phi$ : filler orientation angle in matrix (model 9),  $v_p$ : effective volume fraction. Other parameters are constant.

maximum packing fraction;  $\phi$ , the volume fraction;  $\phi_c$  the percolation threshold;  $\gamma_{pf}$ , the interfacial tension; and  $A$  and  $B$ , constants. The value  $k$  is dependent upon the filler volume fraction, percolation threshold, and surface energy.

It was characterized that few models can successfully predict the electrical conductivity of the composites on the full range of filler percentage. Some models such as Kirkpatrick–Zallen’s model cannot predict the conductivity of composite before the percola-

tion threshold. In addition, some models are dependent on parameters that are not easily accessible. For example, Weber’s model depends on the orientation angle of filler in the matrix. This parameter is not easily calculable and thus makes a great error in the calculations. Another flaw that is observable in thermodynamic models is that the electrical conductivity of composite has been correlated with the surface energy of filler  $\gamma_f$  and polymer  $\gamma_p$  (that indicates to the wettability between filler

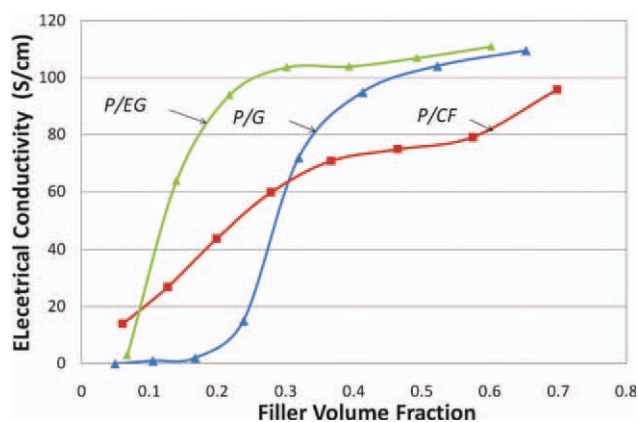


**Figure 2.** The curves of electrical conductivity vs. filler volume fraction for P/G, P/EG, P/CF composites manufactured in this research. [Color figure can be viewed in the online issue, which is available at [wileyonlinelibrary.com](http://wileyonlinelibrary.com).]

and polymer), while the characteristic of wettability between filler and polymer is  $\cos(\theta)$  not surface energy. In other words, the surface energy of filler or polymer cannot individually indicate the goodness of wettability, but also  $\cos(\theta)$  can elucidate this feature. Therefore, it is more accurate to use  $\cos(\theta)$  instead of surface energy. Another limitation in the most models is the limitation of filler type.

It should be emphasized that, the most available models are applicable only for certain fillers. There are few models upon electrical conductivity of composites, which take into account many factors affecting composite conductivity. Most of models follow the simple mixture rules or power-law and contain little flexibility upon various composites data. Therefore, the creation of other models via new approaches seems necessary. However, due to large variety of parameters affecting the electrical conductivity, providing a comprehensive model is difficult. Using a new approach, this research is an attempt to introduce a model, which in addition to the simplicity and availability of model's components can perfectly predict the electrical conductivity of polymer (P)/carbon composites. Another object of this research is that the proposed model can be used for a wider range of filler types.

## EXPERIMENTAL

The polymer resin used in this research is the novalac that is a type of phenolic resin in powder form with 60  $\mu\text{m}$  size and was purchased from Resitan Co. Ltd. The electrical conductivity of phenolic resin is  $\approx 10^{-15}$  S/cm.<sup>24</sup> The graphite (G) powder was purchased from Merck Co. Ltd., containing size  $< 50$   $\mu\text{m}$  and the bulk density of 20–30 g/(100 mL). The expandable graphite and carbon fiber (CF) were purchased from Qingdao Yanxin Graphite Products Co., Ltd and Highborn International Co., Ltd, respectively. In order to prepare the expanded graphite from the expandable graphite, the graphite was placed in furnace 1000°C for 2 min to expand up to 120 times. The dimensions of CF elements were 3 mm length and 15  $\mu\text{m}$  diameter. The bulk densities of G, EG, CF, and phenolic resin were considered 2.35, 1.7, 1.9, and 1.1 g/cm<sup>3</sup>. In this research, the single-filler composites were manufactured by using the phenolic resin as binder and G, EG, and CF

as fillers. The filler contents were 10, 20, 30, 40, 50, 60, 70, and 80 wt %. In order to cure the composites, those were pressed in a three-part-die surrounded by a heating element. The die temperature, pressing pressure, and delaying time were considered 200°C, 230 bar, and 50 min, respectively. In this model, the electrical conductivity of fillers G, EG, and CF were considered 250, 1000, and 598 S/cm, respectively, that were selected from another reference.<sup>14</sup> The electrical conductivity of composites was measured by a home-made method as followed in other paper.<sup>25</sup> The sample dimension was 10  $\times$  10  $\times$  2.5 mm<sup>3</sup>. The two parallel surfaces of composite were covered with the conductive silver adhesive paste. Then the electrodes were fixed on these surfaces. The digital milli-voltmeter and micro-amperemeter were placed in a circuit and connected on these surfaces. The voltage was changed from 0 to 2.9 V, then the slope of the voltage–current ( $V$ - $I$ ) curve equaled the resistance. Resistivity ( $\rho$ ) and conductivity ( $\sigma$ ) are defined as:

$$\sigma = \frac{l}{\rho} = \frac{l}{R.A} \quad (6)$$

$l$  is length and  $A$  is the surface area of the sample.

In order to determine the final formula and constant parameters of formula, the fitting option of MATLAB software was used.

## DISCUSSION ON MANUFACTURED COMPOSITES

In this research, some composites were manufactured by using phenolic resin as binder and CF, EG, and G as fillers. The results of the electrical conductivity via filler volume fraction have been shown in Figure 2. It is noteworthy that the percolation threshold increases from P/CF (at 10 wt % filler), P/EG (at 12 wt %) to P/G (40 wt %). While the maximum electrical conductivity for P/CF (100 S/cm) is lower than P/G (108 S/cm) and P/EG (110 S/cm). The reason of these observations is that the percolation threshold is mainly affected by aspect ratio of filler. Whatever the aspect ratio of fillers increases, the electrical conductivity of composite increases (the aspect ratio of fillers increases from G, EG to CF). While, the maximum electrical conductivity of this curve predominantly depends on purity and electrical conductivity of filler. Because in high filler loadings the electrical conductivity of composite approaches to filler electrical conductivity. Figures 3 and 4 confirm the above mentioned. SEM micrographs in Figure 3 shows that the aspect ratio of fillers increases from G, EG to CF. This property leads to decreasing percolation threshold in P/G, P/EG to P/CF. Figure 4 shows the optical micrographs of P/50 G (a, b), P/50EG (c, d), and P/50CF (e, f). The right figures (a, c, e) are related to the cross-section view of the composite disk and the left figures (b, d, f) are related to the surface-section view. Based on Figure 4, there are essential differences between the morphology of CF, G, and EG, which considerably affect the electrical and mechanical properties of their composites. Figure 4(a, b) show that the graphite contains separate particles in the composite. In the cross-section, these particles appear to be slightly more elongated than those in the surface-section. It can be observed that

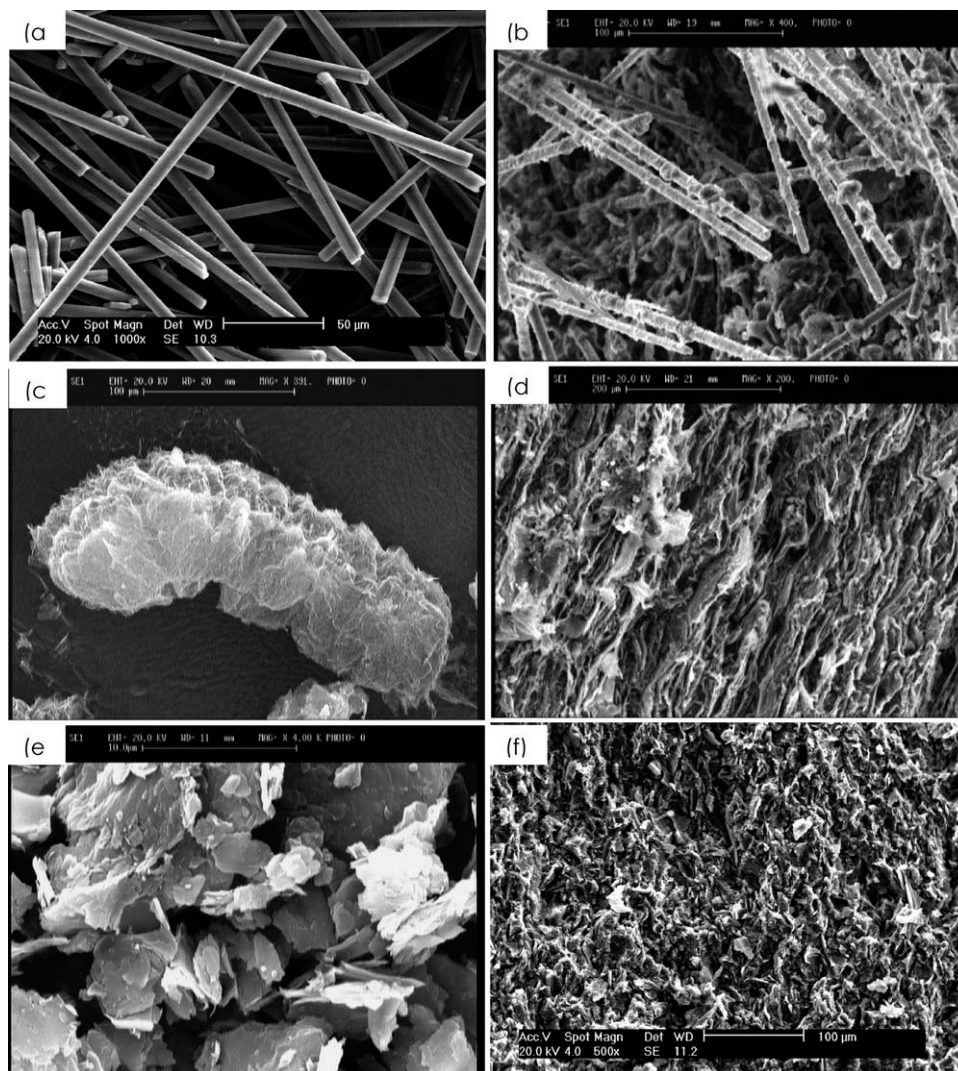


**Figure 3.** SEM micrographs of: (a) pure CF, (b) P/50CF, (c) pure EG, (d) P/50EG, (e) pure G, and (f) P/50 G.

G particles in both cross- and surface sections are discrete. Figure 4(c, d) show that EG particles occupy a greater volume in the composite, as compared with G in such a way that, their layers have been stretched throughout the composite. It can be seen that the compact layers of EG have formed continuous chains in the composite. These chains result in better formation of conductive networks through the composite bulk. Therefore, it is expected that EG is a filler suitable for increasing composite electrical conductivity. CF contains a fibrous shape with a high aspect ratio ( $\approx 150$ ). As can be seen in Figure 4(e, f), the fibers have formed a random orientation in the composite bulk. The high aspect ratio of the fillers facilitates the formation of the conductive network and consequently decreases the percolation threshold. However, the increase of the filler aspect ratio leads to the increasing of the entanglement and agglomeration of the fillers in the composite. These agglomerations create the micro- and nano-sized porosities in the bulk and consequently increase the gas permeation in the composite. In Figure 4(f) a micro-size cavity with 80  $\mu\text{m}$  length is observed.

## MODEL DESCRIPTION

The most important factor that affects the electrical conductivity of composite is filler volume fraction. The percolation threshold region usually appears in the curve of the electrical conductivity vs. volume fraction that this phenomenon makes an S-shape appearance to this curve. In this research, the sigmoidal formula was considered as basic function between electrical conductivity of composite and filler volume fraction. The main reason of this selection is this fact that sigmoidal function with four constant parameters can properly simulate this S-shape form and has high flexibility to the similar shapes. This formula comprises four constant parameters  $a$ ,  $b$ ,  $c$ , and  $d$  that varying these parameters can change the situation of the curve into the desired shape to fit better on the experimental data. Another feature of this formula is that, in spite of some other models, it is able to predict the electrical conductivity for the entire range of filler loading. The sigmoidal function is as follows:

$$y = f(x) = \frac{a}{c + \exp(-bx + d)} \quad (7)$$

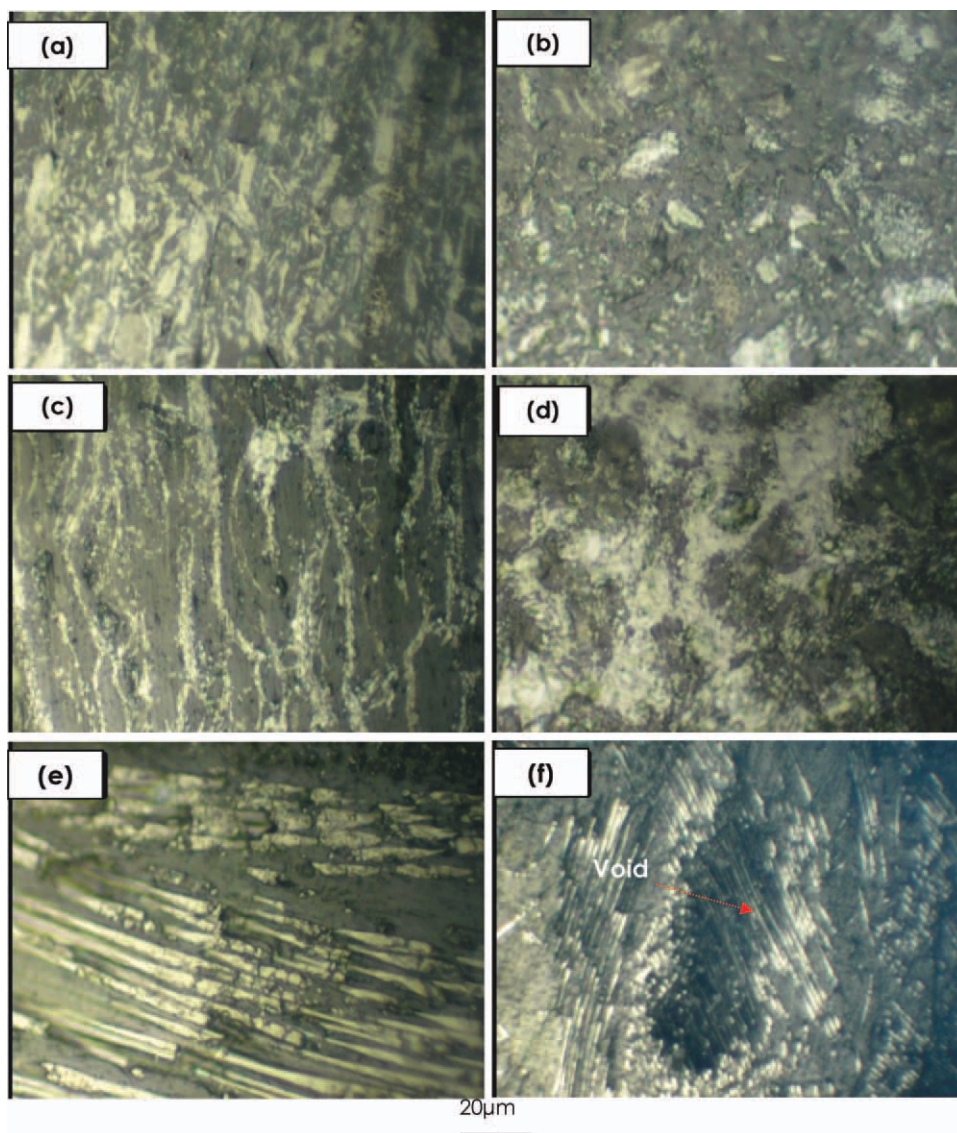


**Figure 4.** Optical micrograph of: P/50 G (a, b), P/EG (c, d), and P/CF (e, f). The right side figures (b, d, and f) are surface-sectional and the left side figures (a, c, and e) are cross-sectional of composite disk. [Color figure can be viewed in the online issue, which is available at [wileyonlinelibrary.com](http://wileyonlinelibrary.com).]

Here  $f(x)$  is electrical conductivity of composite and  $x$  is filler volume fraction. Figure 5 describes the effect of each constant parameters  $a$ ,  $b$ ,  $c$ , and  $d$  on sigmoidal function.

As it was mentioned that the electrical conductivity of polymer-based composite besides the filler volume fraction depends on the other factors such as polymer wettability, filler aspect ratio, filler conductivity, and filler contact resistance (the polymer conductivity is supposed zero, therefore it is not accounted for the model). Therefore, these factors should be placed on the suitable sites in the sigmoidal function. In other words, these factors should be replaced on one of the constant parameters  $a$ ,  $b$ ,  $c$ , and  $d$ . Our approach to perform this issue is that at first, the effect of each effective factor on electrical conductivity of composite is analyzed. Then, regarding the effect of  $a$ ,  $b$ ,  $c$ , and  $d$  on  $f(x)$  [eq. (7)], the appropriate site of each effective factor can be specified. The mentioned approach can be summarized as follows:

- To specify the effect of each constant parameter on the electrical conductivity of composite or  $f(x)$ .
- To find the effect of effective factors such as polymer wettability, filler aspect ratio, filler conductivity, and filler contact resistance on the electrical conductivity of composite to replace these factors on  $a$ ,  $b$ ,  $c$ , and  $d$ .
- To place the effective factors instead of  $a$ ,  $b$ ,  $c$ , and  $d$ , so that an appropriate correlation between effective factors and electrical conductivity [ $f(x)$  in eq. (7)] is made.
- To insert some adjustable parameters into the formula to increase the degree of matching between the experimental and the model data.

The effect of each constant parameter on  $f(x)$  in sigmoidal function is abbreviated as below (Figure 5):

1. Parameter ( $a$ ): when ( $a$ ) increases, the maximum of curve shifts to upper.

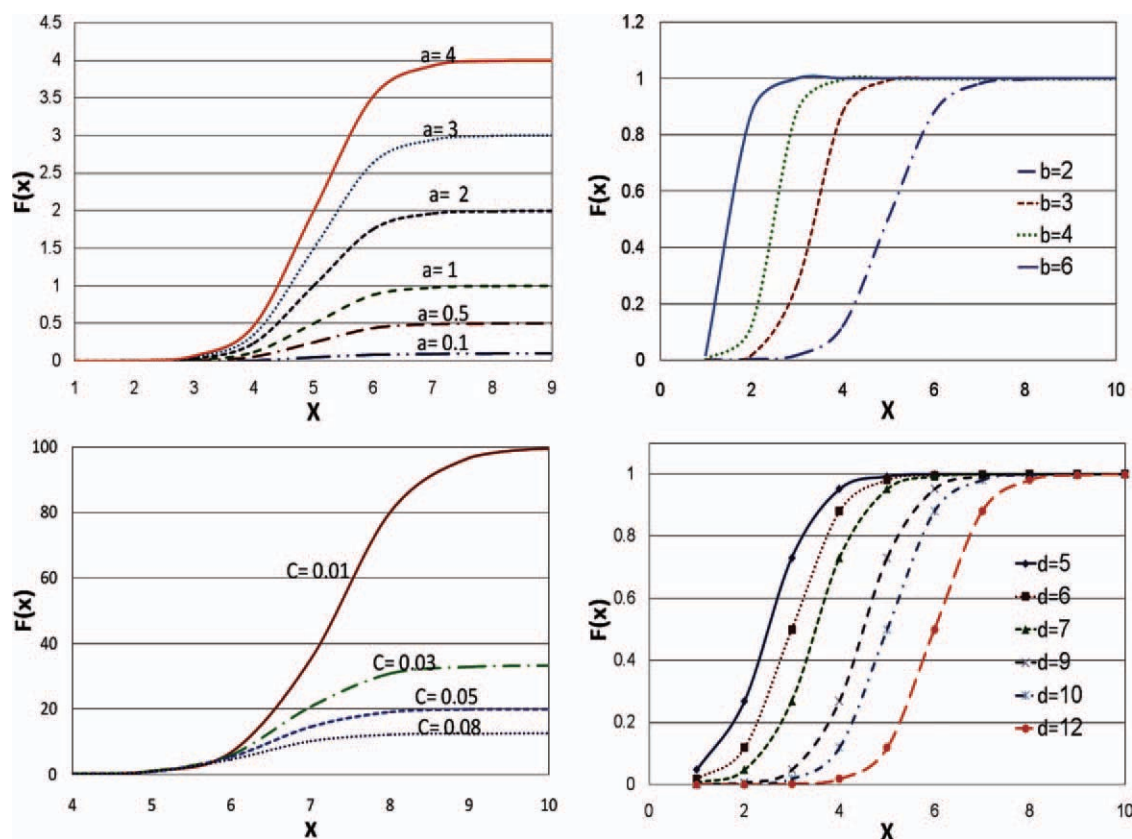


**Figure 5.** The impact of four parameters  $a$ ,  $b$ ,  $c$ , and  $d$  on the curve of sigmoidal function value ( $f(x)$ ) vs. filler volume fraction value ( $x$ ). [Color figure can be viewed in the online issue, which is available at [wileyonlinelibrary.com](http://wileyonlinelibrary.com).]

- Parameter ( $b$ ): when ( $b$ ) increases the curve shifts to the left and the slope curve increases.
- Parameter ( $c$ ): when ( $c$ ) increases, the maximum of the curve decreases.
- Parameter ( $d$ ): when ( $d$ ) increases, the curve shifts to the right.

In this model, four effective factors on the electrical conductivity are to be accounted: filler electrical conductivity, filler aspect ratio, polymer wettability, and contact resistance among the fillers. Below the effect of each parameter on composite conductivity or  $f(x)$  are assessed.

### EFFECTIVE FACTORS ON ELECTRICAL CONDUCTIVITY OF COMPOSITES

#### Electrical Conductivity of Filler

Fillers have different carbon purity and there are often structural anisotropy in common fillers such as carbon black (CB), CF, CNT (carbon nanotube), G, and expanded graphite (EG), which can affect the electrical conductivity of their composites. For example, the acrylonitrile-based CF contains 95 wt % carbon whose graphitic hexagonals have been stretched in longitudinal direction [Figure 3(a)]. Thus, the electrical conductivity of CF along longitudinal is  $598 \text{ S/cm}^{14}$  that is very lower than in-plane electrical conductivity of G ( $5000 \text{ S/cm}$ ). However, the through-plane electrical conductivity of G is as low as  $50 \text{ S/cm}$

that is resulted from Van der Waals bond between graphite layers [Figure 3(e)]. This weak bond inhibits electron passage from one layer to another layer and decreases the mean free path of electrons. The EG particles containing a large graphitic layers are placed on each other and create a warm-like appearance to the EG particle [Figure 3(c)]. When these particles arrange within the composite, form the long chains [Figure 3(d)] that is an important factor in increasing the electrical conductivity of composites. While the G particles are plate-like and create the discrete particles within composite. This is the reason that P/EG have a higher electrical conductivity and lower percolation threshold than P/G.<sup>26</sup> The electrical conductivity of filler directly affects the electrical conductivity of composite. In P/CF, it has been observed that the electrical conductivity of P/CF has a linear relationship with filler conductivity ( $\sigma_f$ ) and filler volume fraction ( $\phi$ ):<sup>27</sup>

$$\sigma_{\max} = \frac{2}{3\pi} \phi \sigma_f \quad (8)$$

It can be observed that on the basis of this relationship that the electrical conductivity of polymer/carbon composites when  $\phi \rightarrow 0$  equals polymer electrical conductivity ( $10^{-14}$  to  $10^{-17} \text{ S/cm}$ )<sup>28</sup> and when  $\phi \rightarrow 1$  approaches to the filler electrical conductivity. Accordingly, it can be concluded that the electrical conductivity of filler has a linear or power-law relationship with electrical conductivity of composite so that by increasing the

filler electrical conductivity, the maximum of sigmoidal curve increases. In this research, the relationship between electrical conductivity of filler and composite has been assumed linear and consequently this factor was placed on the site of parameter (a).

### Aspect Ratio

One of the most important factors affecting percolation threshold is filler aspect ratio. The increase of filler aspect ratio makes it easier to form conductive network and thereby decreasing percolation threshold.<sup>16</sup> The effect of aspect ratio is more evident in the low filler loadings.<sup>29</sup> Taipalus et al.<sup>15</sup> reported that the increase of CF length causes the percolation threshold to decrease and maximum electrical conductivity to increase. Tso-tra and Friedrich<sup>30</sup> has reported the same results for epoxy polymer/CF in different lengths of CF. Sohi et al.<sup>31</sup> reported that the percolation threshold of composites consists of ethylene vinyl acetate copolymer and CB, short CF, and multi wall carbon nanotube (MWCNT) have resulted in 30, 15 and 5 wt %, respectively. The aspect ratio of CB, CF, and MWCNT increases, respectively. This leads to increase of electrical conductivity of percolation threshold from P/CB ( $2.5 \times 10^{-6}$  S/cm), P/CF ( $5 \times 10^{-5}$  S/cm) to P/MWCNT ( $2.5 \times 10^{-4}$  S/cm), respectively and also increasing the curve slope of electrical conductivity vs. filler percentage from CB, CF to MWCNT.<sup>31</sup> Buys et al.<sup>32</sup> attained the same results about CB, CF, and MWCNT composite with PMMA polymer. It was reported that the greater the surface-to-volume ratio of the filler particle, the more likely is inter-particle contact.<sup>16</sup> The higher surface-to-volume ratio of the fibrous filler leads to better increasing the particle-to-particle contact and thus more decreasing electrical resistance in the fiber aggregates in the composite compared with the particulate carbon black. Jana<sup>29</sup> studied on the Hall effect reported that the increasing aspect ratio in CF leads to increasing the mobile carrier concentration. Therefore, the effects of these mobile carriers by CF resulted in increasing electrical conductivity. It was reported that increasing aspect ratio of CB led to decreasing percolation threshold and increasing the slope of conductivity/filler curve in P/CB with respect to P/G.<sup>33</sup> Iosif<sup>34</sup> reported that the increase of aspect ratio in MWCNT resulted in decreasing percolation threshold and increasing the maximum of electrical conductivity of composite. Carter<sup>16</sup> and Clingerman<sup>35</sup> also confirmed the above findings. Therefore, based on experimental tests, it can be concluded that the increase of aspect ratio decreases the percolation threshold (leads to the sigmoidal curve shifts to the left side), increases the slope of sigmoidal curve, and increases maximum value of sigmoidal curve. Thus, this factor was placed in site of parameters (a) and (b).

### Surface Energy

Surface energies of polymer and filler determine the wettability of filler by polymer. The wettability can affect the filler agglomeration, filler distribution, composite porosity and, thereby affecting the electrical conductivity of the composite.<sup>1,36,37</sup> When the wettability is of high value, the polymer surrounds each filler, inhibits the direct contact between fillers, and consequently decreases electrical conductivity of composite. In addition, the high wettability leads to decreasing agglomeration<sup>38</sup> and the fillers highly distribute within the matrix. This fillers

configuration within matrix is not suitable for electrical conductivity of composite, because according to Figure 6 the conductive network is formed in a weak distribution and high dispersion state. In other words, some agglomeration between fillers is necessary to increase the electrical conductivity of composite and in this filler arrangement, the conductive networks can be more properly formed.<sup>29</sup> The equations to calculate the surface energy is as follows:<sup>38</sup>

$$\cos(\theta) = \frac{\gamma_s - \gamma_{SL}}{\gamma_L} \quad (9)$$

$$\gamma_{SL} = \gamma_s + \gamma_L - 2(\gamma_s \cdot \gamma_L)^{0.5} \quad (10)$$

$\gamma_s$ ,  $\gamma_L$ ,  $\gamma_{SL}$ , and  $\theta$  are the surface energies of filler, polymer, filler/polymer, and wetting angle. The symbol of polymer wettability is  $\cos(\theta)$ . As eq. (9), smaller differences between the two surface energies of filler and polymer lead to the better wetting of the filler by the polymer (or low wetting angle). It is for this reason that a somewhat larger difference between the surface energy of the filler and the polymer is desirable.<sup>11</sup>

**Calculation of Wetting Angle in Manufactured Composites.** Usually the wetting angle between carbon-based fillers and common polymers is from 35° to 70°. Phenolic resin contains the highest surface energy in comparison to other common polymers (Table II). Thus, the highest wetting angle is related to phenolic resin. The wetting angle between phenolic resin and CF is as follows:

$$\begin{aligned} \gamma_{ls} &= \gamma_l + \gamma_s - 2(\gamma_l \times \gamma_s)^{0.5} = 52 + 28.89 - 2(52 \times 28.89)^{0.5} = 3.371 \\ \cos \theta &= 0.49 \rightarrow \theta = 60.65^\circ \quad (12) \end{aligned}$$

Wetting angle between phenolic resin and G is as follows:

$$\begin{aligned} \gamma_{ls} &= \gamma_l + \gamma_s - 2(\gamma_l \times \gamma_s)^{0.5} = 52 + 24 - 2(52 \times 24)^{0.5} = 5.34 \\ \cos \theta &= 0.35 \rightarrow \theta = 68.9^\circ \quad (13) \end{aligned}$$

Accordingly, the wetting angle for polyamide/G and nylon/G are calculated 56° and 45°, respectively, that are very lower than that of phenolic/G.

In this model, it is assumed that the surface energy influences the orientation of fillers in the matrix so that by decreasing  $\cos(\theta)$ , the electrical conductivity of composite increases. Therefore, this term has been placed instead of parameter (d).

### Interface Contact Resistance

There is a considerable resistance over the passage of electrons crossing from one filler to another filler that is named "interface contact resistance." The interface contact surface among the fillers in comparison with the bulk contains a higher resistivity value. This resistance remarkably depends on filler particle size, surface chemistry of fillers,<sup>16</sup> filler asperity,<sup>35</sup> and filler roughness.<sup>40,41</sup> The interface contact resistance between fillers directly affects tunneling effect (the dominant mechanism upon creating conductivity before percolation threshold), electron hopping, and electric field radiation mechanisms (the dominant mechanism upon creating conductivity in high filler loadings in which the direct contact among fillers is made).<sup>16,38,42-44</sup>



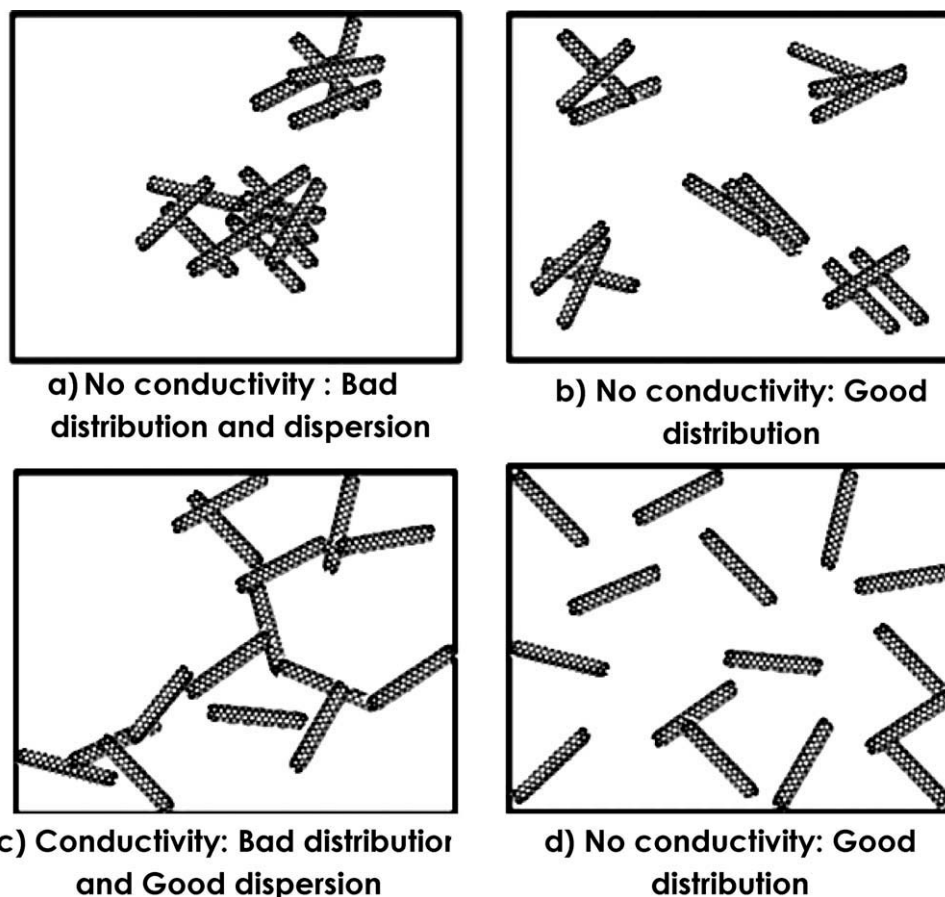


Figure 6. The effect of filler arrangement on composite electrical conductivity.<sup>16</sup>

Whenever the particle size increases, the contact resistance among fillers decreases and thereby increasing electrical conductivity of composite. Hui et al.<sup>45</sup> studied the influence of graphite particle size on the electrical conductivity of composite bipolar plates. According to these results, the electrical conductivity of novalac/G increases by increasing the graphite particle size. Shen et al.<sup>46,47</sup> and Maheshwari et al.<sup>48</sup> in individual researches showed that increasing particle size resulted in higher electrical conductivity of composites. The experimental calculation of contact resistance among filler particles is not an easy way. Therefore, this parameter is usually calculated by theoretical method. Some authors for simplicity consider this parameter as a fitting factor.<sup>49</sup> For carbon nanotubes with electrical conductivity in the range of  $10^4$ – $10^7$  S/cm, the contact resistance is in the range of 40–100 k $\Omega$ . But the theoretical calculations shows that the contact resistance between nanotubes can vary from 100 k $\Omega$  to 3.4 M $\Omega$  and is strongly dependent on the atomic structures in the contact region, contact length, nanotube diameter, and the structural relaxation of the nanotubes.<sup>50</sup> Depending on the kind of filler, the diameter, interface area, matrix properties, and the film thickness the range of this resistance would vary from  $10^2$  to  $10^{16}$  k $\Omega$ . Yang et al.<sup>49</sup> took into account the value of contact resistance between CNTs 6.1 k $\Omega$ . In this research, the contact resistance values related to all filler types were considered between 0 and 1 k $\Omega$ . According to above

Table II. Room Temperature Surface Energy Values of Polymers and Fillers Used for Testing the Model<sup>14,29,39</sup>

Polymer	Surface energy (mJ/m <sup>2</sup> )
Phenolic resin	52
Polyethylene	31
Polypropylene	33
PES	36
Polyurethane	40
PMMA	28
Nylon 6/6	41
Poly liquid crystal (LCP)	36
Polyester	32
Nitrile rubber	49
Venyle ester	36
Polystyrene	41
Epoxy resin	47
Carbon fiber	29
Expanded graphite	24
Graphite	24

**Table III.** The Results of Model Testing Step by Experimental Data via Fitting Option of MATLAB Software

Reference	Filler	Polymer	$\sigma_f$ (S/cm)	AR	CR (k $\Omega$ )	Cos ( $\theta$ )	R-square	Adj. R-square	SSE	RMSE
My work	G	Phenolic	250	0.040	0.87	0.35	0.9978	0.9969	38	2.76
Kang et al. <sup>38</sup>	G	Phenolic	400	0.040	0.17	0.35	0.9998	0.9998	0.1603	0.13
Dweiri and Sahari <sup>36</sup>	G	Polypropylene	300	1.38	0.58	0.789	0.9998	0.9998	0.1603	0.1334
Otieno and Kim <sup>51</sup>	G	Polyurethane	300	0.36	0.79	0.5	1	1	4 e-009	4 e-5
Kuan et al. <sup>52</sup>	G	Vinyl ester	250	0.72	0.41	0.65	0.9909	0.9864	0.0003	0.0086
Yin et al. <sup>53</sup>	G	Phenolic	250	3.9	0.59	0.35	0.9941	0.9912	182.4	6.75
Carter <sup>14</sup>	G	LCP	300	2.11	0.39	0.63	0.9971	0.9967	0.86	0.25
Keith et al. <sup>5</sup>	G	Polypropylene	400	1.62	0.35	0.78	1	1	0.0008	0.0078
My work	CF	Phenolic	590	202	0.24	0.49	0.9856	0.9799	78	3.9
Pramanik et al. <sup>16</sup>	CF	Nitrile rubber	598	50	0.12	0.5	0.997	0.996	0.02658	0.066
Jimenez and Jana <sup>54</sup>	CF	PMMA	600	81.37	0.47	0.51	0.9996	0.9994	1.655 e-7	0.00016
Vilcakova et al. <sup>55</sup>	CF	Polyester	590	136.6	0.26	0.62	0.9512	0.9447	0.002813	0.0137
Carter <sup>14</sup>	CF	LCP	598	202	0.52	0.78	0.9969	0.9962	0.1239	0.1173
My work	EG	Phenolic	1000	107.5	0.10	0.35	0.9782	0.9673	179	6.6
Jin et al. <sup>56</sup>	EG	PES	1000	11.54	0.18	0.47	1	1	2 e-10	7 e-6
Chen et al. <sup>57</sup>	EG	Vinyl ester	1000	7.37	0.24	0.47	0.9936	0.9903	109.9	5.242
Zhang et al. <sup>58</sup>	EG	Phenolic	1000	821.3	0.47	0.35	0.9435	0.9247	0.000118	0.0044
Sengupta et al. <sup>59</sup>	EG	Polystyrene	1000	22.22	0.21	0.41	1	1	7 e-11	4 e-6
Kalaitzidou et al. <sup>60</sup>	EG	Polypropylene	1000	11.03	0.79	0.78	1	1	2 e-7	0.00018

mentioned, by increasing the contact resistance among fillers, the electrical conductivity of composite decreases or the maximum electrical conductivity in sigmoidal curve decreases. Therefore, the contact resistance factor would be placed in the site of parameter ( $a$ ).

### MODEL ASSUMPTIONS

In this model, the interaction among effective factors (aspect ratio, wettability, etc.) is ignored and the temperature is assumed constant. In this approach, it has been tried to consider a simple relationship between effective factors and conductivity of composite ( $f(x)$ ). It seems more research is needed for the functions which are more complex. In addition, this should be mentioned that this model is proposed for polymer-based carbon composites such as P/G, P/EG, and P/CF and is not recommended for metallic-based composites. In addition, the sigmoidal formula cannot be exactly fitted upon the curve of P/CNT composites. The reason of this fact is that the composites including the polymer and CNT usually have very low percolation threshold that is not clearly observable on the curve.

### CURVE FITTING QUALITY

The curve fitting option of MATLAB software used for modeling introduces four factors for checking the quality of fittings. These four parameters and their formulations derived from MATLAB help are as follows:

- Sum of squares due to error (SSE). This statistic measures the total deviation of the response values from the fit to the

response values. It is also called the summed square of residuals.

$$SSE = \sum_{i=1}^n (y_i - \hat{y}_i)^2 \quad (13)$$

$y_i$ ,  $\hat{y}_i$ , and  $n$  are the experimental value, the predicted response value, and the number of response values, respectively. A value closer to 0 indicates that the model has a smaller random error component, and that the fit will be more useful for prediction.

- R-square. R-square statistic measures how successful the fit is in explaining the variation of the data. Putting another way, R-square is the square of the correlation between the response values and the predicted response values. R-square is defined as the ratio of the sum of squares of the regression (SSR) and the total sum of squares (SST). SSR is defined as:

$$SSR = \sum_{i=1}^n (\hat{y}_i - \bar{y})^2 \quad (14)$$

$\bar{y}$  is the average of the data set. SST is also called the sum of squares about the mean, and is defined as:

$$SST = \sum_{i=1}^n (y_i - \bar{y})^2 \quad (15)$$

where  $SST = SSR + SSE$ . Given these definitions, R-square is expressed as:

**Table IV.** The Adjustable Parameters Related to Prepared Composites Applied for Model Testing

Adjustable parameters	P/G	P/EG	P/CF
$a_0$	0.09	$1.6 \times 10^{-5}$	$1 \times 10^{-6}$
$b_0$	166.2	0.13	0.072
$c_0$	-14.47	-13.23	-34.72

$$R\text{-square} = \frac{SSR}{SST} = 1 - \frac{SSE}{SST} \quad (16)$$

$R$ -square can take on any value between 0 and 1, with a value closer to 1 indicating that a greater proportion of variance is accounted for by the model. For example, an  $R$ -square value of 0.8234 means that the fit explains 82.34% of the total variation in the data about the average.

- Adjusted  $R$ -square or degrees of freedom. This statistic uses the  $R$ -square statistic defined above and adjusts it based on the residual degrees of freedom. The residual degree of freedom is defined as the number of response values ( $n$ ) minus the number of fitted coefficients ( $m$ ) estimated from the response values.

$$v = n - m \quad (17)$$

$v$  indicates the number of independent pieces of information involving the  $n$  data points that are required to calculate the sum of squares. Note that if parameters are bounded and one or more of the estimates are at their bounds, then those estimates are regarded as fixed. According to MATLAB help, the adjusted  $R$ -square statistic is generally the best indicator of the fit quality when two models that are nested are compared. The adjusted  $R$ -square statistic can take on any value less than or equal to 1, with a value closer to 1 indicating a better fit.

- Root mean squared error (RMSE). This statistic is also known as the fit standard error and the standard error of the regression. It is an estimate of the standard deviation of the random component in the data, and is defined as:

$$RMSE = s = \sqrt{MSE} \quad (18)$$

where MSE is the mean square error or the residual mean square:

$$MSE = \frac{SSE}{v} \quad (19)$$

Just as with SSE, an MSE value closer to 0 indicates a fit that is more useful for prediction.

## INTRODUCTION OF THE FUNCTION

In this research, the electrical conductivity of composite ( $\sigma_{\text{composite}}$ ) is related to filler volume fraction( $x$ ) by a sigmoidal function. In addition, four other effective factors including filler electrical conductivity ( $\sigma_f$ ), filler aspect ratio (AR), surface

energy ( $\cos\theta$ ), and interface contact resistance among fillers (CR) are inserted into this function. These extra factors are placed on the special site of the sigmoidal function as follows:

- The factor of " $\sigma_f$ " is placed upon the site of parameter ( $a$ ).
- The factor of "AR" is placed upon the site of parameters ( $a$ ) and ( $b$ ).
- The factor of " $\cos\theta$ " is placed upon parameter ( $d$ ).
- The factor of "CR" is placed upon parameter ( $a$ ).

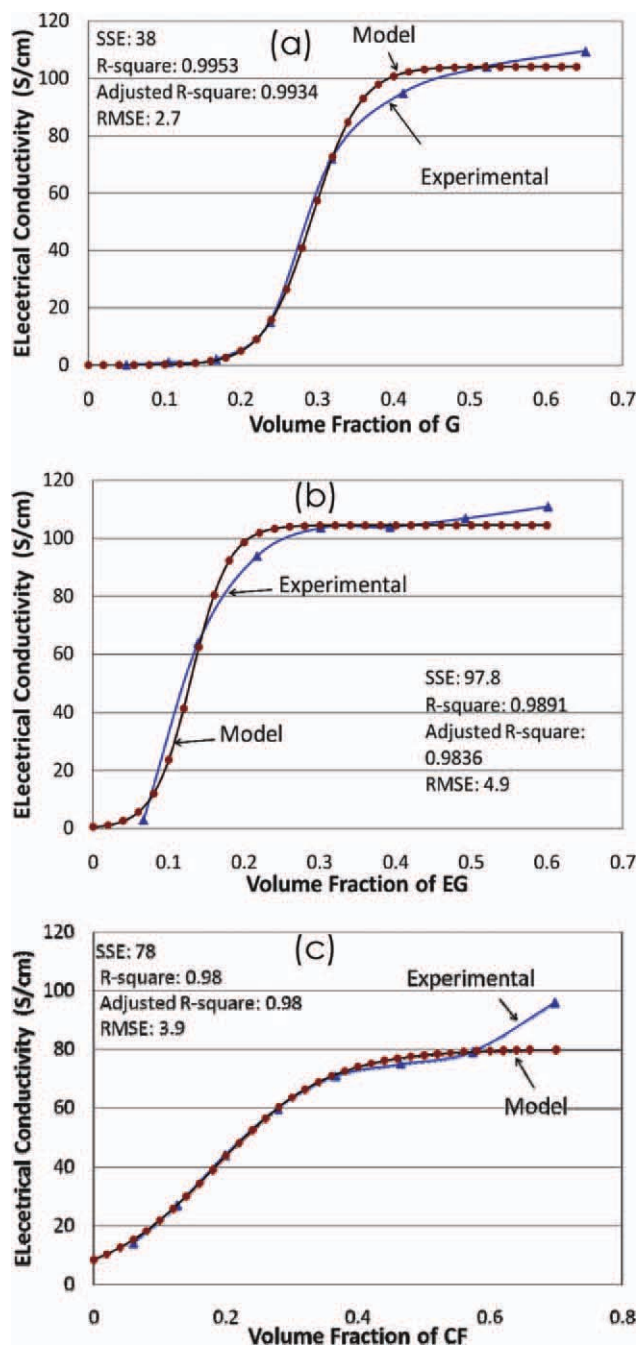


**Figure 7.** Comparison model with experimental data related to manufactured composites in this research; (a) P/G, (b) P/EG, and (c) P/CF. [Color figure can be viewed in the online issue, which is available at [wileyonlinelibrary.com](http://wileyonlinelibrary.com).]

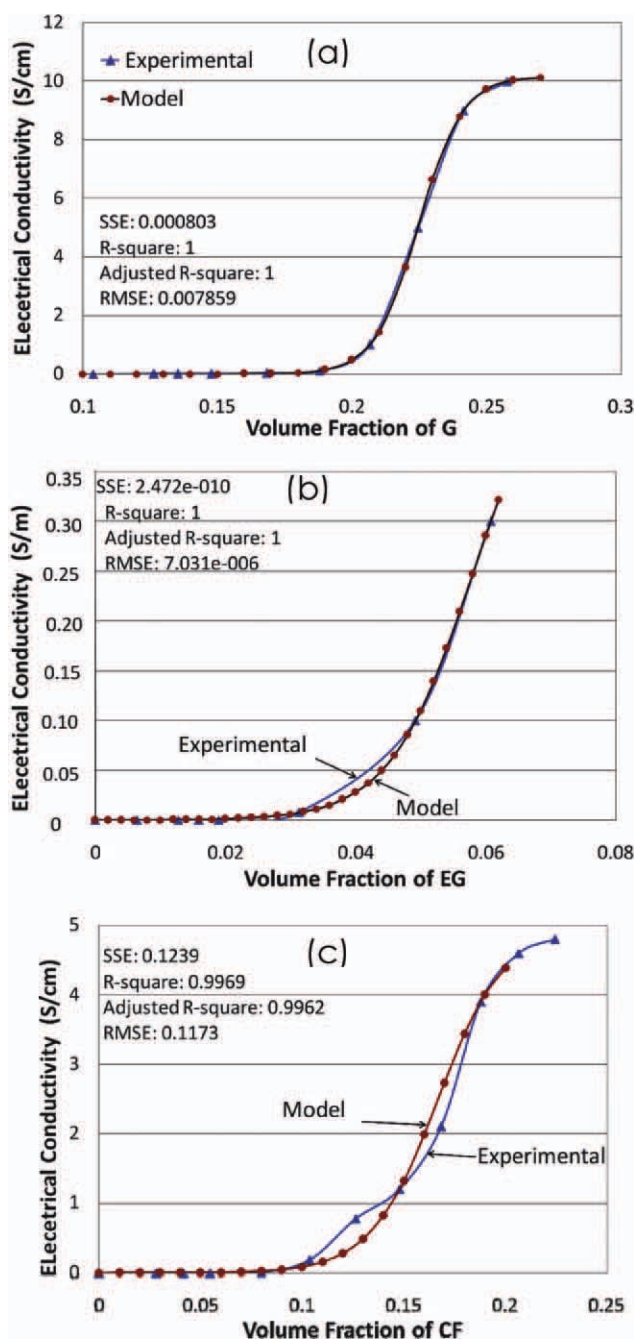


**Figure 8.** Comparison model with experimental data related to others' composites: (a) P/G,<sup>5</sup> (b) P/EG,<sup>56</sup> and (c) P/CF.<sup>14</sup> [Color figure can be viewed in the online issue, which is available at [wileyonlinelibrary.com](http://wileyonlinelibrary.com).]

According to above, the final formula is as follows:

$$\sigma_{\text{composite}} = \frac{a_0 \times \frac{AR}{CR} \sigma_f}{0.01089 + \exp(-b_0 \times AR \cdot x + d_0 \times \cos \theta)}$$

$$\cos(\theta) = \frac{\gamma_S - \gamma_{SL}}{\gamma_L}$$

$$\gamma_{SL} = \gamma_S + \gamma_L - 2(\gamma_S \cdot \gamma_L)^{0.5} \quad (20)$$

The model was introduced into the MATLAB software to achieve the constant parameters, fitness coefficient, and fitness

quality. Three constant parameters  $a_0$ ,  $b_0$ , and  $c_0$  are considered as adjustable parameters. These parameters are calculated by fitting the model on experimental data.

The testing step of the model was performed by 19 experimental samples illustrated in Table III. It should be noted that the  $\sigma_f$  were selected based on corresponding references. The  $\sigma_f$  values of G 250, 300 and 400, EG 1000, and CF 600 were selected. AR values were selected based on corresponding references. The interface contact resistance values (CR) were presupposed between 0.1 and 0.9 k $\Omega$ .<sup>49,50</sup> The  $\cos(\theta)$  were calculated by using eqs. (9) and (10) and the data of Table II.

Table III shows that there is a significant agreement between experimental and model responses. It can be observed that the values of  $R$ -square and adjusted  $R$ -square (as the best indicator of the fit quality) are equal to 1 or very close to 1. In addition, the SSE and RMSE values are insignificant. This indicates that there is very suitable agreement between experimental and model data and the function gives good responses to the data related to different composites. Table IV indicates the adjustable parameters values  $a_0$ ,  $b_0$ , and  $c_0$ . Figures 7 and 8 obviously show the good agreement between the model and experimental data upon the manufactured composites and other composites, respectively. Consequently, it can be concluded that the prepared function can be used for prediction of electrical conductivity of polymer-based carbon composites. Of course, further research is under consideration to improve the model.

## CONCLUSIONS

In this research, one statistical-thermodynamic model was introduced for prediction of electrical conductivity of polymer-based carbon composites, such as P/G, P/EG and P/CF, used for bipolar plate of proton exchange membrane fuel cell. In this model, the correlation between the electrical conductivity of composite and filler volume fraction was assumed in accordance to sigmoidal function and then some other effective factors such as the electrical conductivity of filler, filler aspect ratio, wettability as well as interface contact resistance, were replaced upon constant parameters of sigmoidal function. The location of each factor in the function depended on how the factors affected the electrical conductivity of composites. In order to test the model, some P/G, P/EG and P/CF composites were manufactured. The test of the model was also performed by some other composites derived from other researches. The fitting quality was assessed by  $R$ -square, adjusted  $R$ -square, SSE, and RMSE parameters. The results of composites testing specified that the  $R$ -square and adjusted  $R$ -square were equal or close to 1 and also the SSE and RMSE values were insignificant which pointed out the fact that there was an acceptable agreement between model and experimental data. A specific difference between the prepared model with other models is that in this model, the electrical conductivity of the composite was correlated with wetting angle, not to surface energy. In addition, in comparison with other models, this model can be used for more types of fillers.

## ACKNOWLEDGMENTS

The financial support for this work was provided by the Material Research Center to doctor Nozad that is gratefully acknowledged.

Also, authors kindly acknowledge Professor Moradi; the Header of coating Lab, in physics faculty in Shiraz University.

## REFERENCES

1. Keith, J. M.; King, J. A.; Barton, R. L. *J. Appl. Polym. Sci.* **2006**, *102*, 3293.
2. Bar-On, I.; Kirchain, R.; Roth, R. *J. Power Sources* **2002**, *109*, 71.
3. King, J. A.; Tucker, K. W.; Meyers, J. D.; Weber, E. H.; Clingerman, M. L.; Ambrosius, K. R. *Polym. Compos.* **2001**, *22*, 142.
4. Heiser, J. A.; King, J. A.; Konell, J. P.; Miskioglu, I.; Sutter, L. L. *J. Appl. Polym. Sci.* **2004**, *91*, 2881.
5. Keith, J. M.; King, J. A.; Johnson, B. A. *J. New Mater. Electrochem. Syst.* **2008**, *11*, 253.
6. McCullough, R. L. *Compos. Sci. Technol.* **1985**, *22*, 81.
7. Weber, M.; Kamal, M. R. *Polym. Compos.* **1997**, *18*, 711.
8. Kirkpatrick, S. *Rev Mod Phys* **1973**, *45*, 574.
9. McLachlan, D. S.; Blaszkiewicz, M.; Newnham, R. E. *J. Am. Ceram. Soc.* **1990**, *73*, 2187.
10. Mclanchlan, D. S. *J. Phys. C Solid State Phys.* **1987**, *20*, 865.
11. Mamunya, P.; Davidenko, V. V.; Lebedev, E. V. *Compos. Interfaces* **1997**, *4*, 169.
12. Mamunya, P.; Davidenko, E.; Lebedev, V. *Dopovidi AN Ukr* **1991**, *5*, 124.
13. Matthew, L.; Clingerman, E. H.; Weber, J. A.; King, K. H. S. *J. Appl. Polym. Sci.* **2003**, *88*, 2280.
14. Carter, R. L. B. Ph.D. Thesis, University of Michigan, King, JA, **2008**.
15. Taipalus, R.; Harmia, T.; Zhang, Q. M.; Friedrich, K. *Compos. Sci. Technol.* **2001**, *61*, 801.
16. Pramanik, P. K.; Khastgir, D.; Saha, T. N. *Compos A* **1991**, *23*, 183.
17. Jing, X.; Zhao, W.; Lan, L. *J. Mater. Sci. Lett.* **2000**, *19*, 377.
18. Gokturk, S. H.; Fiske, T.; Kalyon, D. M. *J. Appl. Polym. Sci.* **1993**, *50*, 1891.
19. Fiske, T.; Gokturk, S. H.; Kalyon, D. M. *J. Mater. Sci.* **1997**, *32*, 5551.
20. Yi, Y.; Choi, J. M. *J. Electroceram.* **1999**, *3*, 361.
21. Mapleston, P. *Mod. Plast. Int.* **1992**, *69*, 80.
22. Lux, F. *J. Mater. Sci.* **1993**, *28*, 285.
23. Zallen, R. *The Physics of Amorphous Solids, The Percolation Model*; Wiley: New York, **1983**.
24. Ratna, D. *Handbook of Thermoset Resins*; iSmithers: United Kingdom, **2009**; Chapter 2, p 70.
25. Taherian, R.; Nozad, A.; Hadianfard, M. *J. Mater. Design.* **2011**, *32*, 3883.
26. Kuilla, T.; Bhadra, S.; Yao, D.; Kim, N. H.; Bose, S.; Lee, J. H. *Prog. Polym. Sci.* **2010**, *35*, 1350.
27. Thongruang, W.; Spontak, R. J.; Balik, C. M. *Polymer.* **2002**, *43*, 2279.
28. Clingerman, M. L.; King, J. A.; Schulz, K. H.; Meyers, J. D. *J. Appl. Polym. Sci.* **2002**, *83*, 1341.
29. Al-Saleh, M. H.; Sundararaj, U. *Carbon* **2009**, *47*, 2.
30. Tsotra, P.; Friedrich, K. *Compos. A* **2003**, *34*, 75.
31. Sohi, N. J. S.; Bhadra, S.; Khastgir, D. *Carbon* **2011**, *49*, 1349.
32. Buys, Y. F.; Aoyama, T.; Akasaka, S.; Asai, S.; Sumita, M. *Compos. Sci. Technol.* **2010**, *70*, 200.
33. Rosca, I. D.; Hoa, S. V. *Carbon* **2009**, *47*, 1958.
34. Dalmas, F.; Dendievel, R.; Chazeau, L.; Cavaillé, J. Y.; Gauthier, C. *Acta. Mater.* **2006**, *54*, 2923.
35. Bahrami, M.; Culham, J. R.; Yovanovich, M. M.; Schneider, G. E. *ASME Appl. Mech. Rev.* **2003**, *59*, 1.
36. Dweiri, R.; Sahari, J. *J. Power Sources* **2007**, *171*, 424.
37. Ezquerra, A.; Connor, T.; Roy, S.; Kuleszcza, M.; Nascimento, J. F.; Calleja, J. B. *Compos. Sci. Technol.* **2001**, *61*, 903.
38. Kang, S. J.; Kim, D. O.; Lee, J. H.; Lee, P. C.; Lee, M. H.; Lee, Y.; Lee, J. Y.; Choi, H. R.; Lee, J. H.; Oh, Y. S. *J. Power Sources* **2010**, *195*, 3794.
39. Petrie, E. M. "Chapter 2: Theories of Adhesion", *Handbook of Adhesives and Sealants*, 2nd ed.; Wiley: New York, **2006**.
40. Bahrami, M.; Yovanovich, M.; Culham, J. *Int. J. Heat. Mass. Transfer.* **2005**, *48*, 3284.
41. Bahrami, M.; Yovanovich, M. M.; Culham, J. R. *J. Thermophys. Heat Transfer* **2007**, *21*, 153.
42. Alexander, M. G. *Mater. Res. Bull.* **1999**, *34*, 603.
43. Psarras, G. *Compos. A* **2006**, *37*, 1545.
44. Allaoui, A.; Hoa, S.; Pugh, M. *Compos. Sci. Technol.* **2008**, *68*, 410.
45. Chen, H.; Liu, H. B.; Yang, L.; Li, J. X. *Int. J. Hydrogen Energy* **2010**, *35*, 3105.
46. Shen, C.; Mu, P.; Yuan, R. *J. Power Sources* **2006**, *162*, 460.
47. Chunhui, S.; Mu, P.; Zhoufa, H.; Runzhang, Y. *J. Power Sources* **2007**, *166*, 419.
48. Maheshwari, H. P.; Mathur, B.; Dhami, L. *J. Power Sources* **2007**, *173*, 394.
49. Yang, D.; Hu, X.; Zhang, Y. S.; Dai, M. *PIERS Online* **2007**, *3*, 457.
50. Buldum, A.; Lu, J. P. *Phys. Rev. B.* **2001**, *63*, 161403.
51. Otieno, G.; Kim, J. *J. Ind. Eng. Chem.* **2008**, *14*, 187.
52. Kuan, H.; Ma, C.; Chen, K.; Chen, S. *J. Power Sources* **2004**, *134*, 7.
53. Yin, Q.; Li, A.; Wang, W.; Xia, L.; Wang, Y. *J. Power Sources* **2007**, *165*, 717.
54. Jimenez, G.; Jana, S. *Compos. A* **2007**, *38*, 983.
55. Vilcakova, J.; Saha, P.; Quadrat, O. *Eur. Polym. J.* **2002**, *38*, 2343.
56. Jin, J.; Leesirisan, S.; Song, M. *Compos. Sci. Technol.* **2010**, *70*, 1544.
57. Chen, W.; Liu, Y.; Xin, Q. *Int. J. Hydrogen Energy* **2010**, *35*, 3783.
58. Zhang, X.; Shen, L.; Xia, X.; Wang, H.; Du, Q. *Mater. Chem. Phys.* **2008**, *111*, 368.
59. Sengupta, R.; Bhattacharya, M.; Bandyopadhyay, S.; Bhowmick, A. K. *Prog. Polym. Sci.* **2011**, *36*, 638.
60. Kalaitzidou, K.; Fukushima, H.; Drzal, L. *Compos. Sci. Technol.* **2007**, *67*, 2045.